African Journal of Biotechnology Vol. 10(14), pp. 2588-2599, 4 April, 2011
Available online at http://www.academicjournals.org/AJB
DOI: 10.5897/AJB10.739
ISSN 1684–5315 © 2011 Academic Journals

Full Length Research Paper

Subcellular localization and expression analysis of the BmDSCLP protein from silkworm, *Bombyx mori*

Jianhong Shu, Bo Liu, Hongxiu Ge, Qingliang Zheng, Zhengbing Lv, Jian Chen, Zuoming Nie, Jianqing Chen, Xiangfu Wu and Yaozhou Zhang*

Institute of Biochemistry, Zhejiang Sci-Tech University, Zhejiang Provincial Key Laboratory of Silkworm Bioreactor and Biomedicine, Hangzhou 310018, China.

Accepted 15 March, 2011

Leucine-rich repeat (LRR) proteins play important roles in the transduction of cellular signals and activation of defense responses. By scanning the cDNA library of silkworm (*Bombyx mori*) pupae constructed in our laboratory, we identified a 1557 bp gene that encodes a protein homologous to the death-associated small cytoplasmic leucine-rich protein, which was named as BmDSCLP. The full-length gene (GenBank accession no. FJ602779) contained a 642 bp open reading frame (ORF) encoding 213 amino acid residues. The ORF of this gene was inserted into the prokaryotic expression vector pET-28a(+) to construct a recombinant expression plasmid and the fusion protein was expressed in *Escherichia coli* BL21(DE3) cells. The fusion protein was purified by Ni-affinity chromatography and fast protein liquid chromatography (FPLC) and its size was then, determined by liquid chromatography-mass spectrometry (LC/MS/MS) and found to be 27.74 kD. Polyclonal antibodies were raised by subcutaneous injection of the recombinant protein into New Zealand white rabbits and the titer reached 1:12800. Analysis of the subcellular localization of the BmDSCLP protein revealed that, the protein was localized in both the cytoplasm and nucleus, but the amount in the former was slightly higher than that in the latter. In addition, real-time fluorescence quantification polymerase chain reaction studies were conducted to investigate *BmDSCLP* transcription at different developmental stages and in different tissues of the fifth instar larva. The results indicated that, *BmDSCLP* is widely transcribed in different stages and tissues of the silkworm. Analysis of stage-specific transcription patterns indicated that, the transcriptional level of *BmDSCLP* was highest in adults and lowest in eggs. Analysis of tissue-specific transcription patterns revealed that, the transcriptional level of *BmDSCLP* was highest in genital organs and lowest in silk glands. These results suggest that BmDSCLP plays important roles in the reproductive development of *B. mori*.

Key words: *Bombyx mori*, death-associated small cytoplasmic leucine-rich protein, prokaryotic expression, fluorescence quantification polymerase chain reaction.

INTRODUCTION

Leucine-rich repeats (LRRs) were originally discovered by Patthy (1987) and are found in proteins from a diverse array of organisms ranging from bacteria and plants to yeast and humans (Buchanan and Gay, 1996). LRR proteins are involved in a broad range of biological activities, including RNAse inhibition (Kobe and Deisenhofer, 1995), GTPase activation (Haberland and Gerke, 1999), protein-protein interactions (Kobe and Deisenhofer, 1994), signal transduction (Medzhitov et al., 1997), transcription (Draper et al., 1994), nervous system growth and development and remodeling (Tensen et al., 1994; Kuja-Panula et al., 2003). Although, the length of LRRs can differ substantially, most contain between 20

*Corresponding author. E-mail: yaozhou@chinagene.com. Tel: 0571-86843198.

and 29 residues, with 24 being the most common. Multiple LRRs are usually present in tandem, with the highest known number (38) found in the plant disease resistance gene Cf-2 (Dixon et al., 1996) and the lowest known number (1) found in platelet glycoprotein IbL (Roth, 1991). The three-dimensional (3D) structure of the LRR present in a complex of porcine ribonuclease inhibitor with ribonuclease has been determined (Kobe and Deisenhofer, 1993; Kobe and Deisenhofer, 1996). The crystal structure shows that, each LRR is composed of a β-sheet and an α-helix. The hairpin-like structure of the LRR is mainly formed by the β-sheet (LxxLxLxxN/CxL) and α-helix (xaxx ± a ± ± ± ± a A ± ± x ± ±) that are connected by a loop ring (Kobe and Kajava, 2001). It is possible that other LRR proteins may have a similar structure in their repeat region.

The death-associated small cytoplasmic leucine-rich protein (DSCLP) family has been studied in various insects and proteins such as toll, slit and connection have been identified in fruit flies (Nose et al., 1994; Rose et al., 1997; Wu et al., 1999). The silkworm (*Bombyx mori*) is an economically important Lepidoptera model insect and is therefore, suitable as a model organism in insect studies. However, there is no report on a lepidopteran DSCLP protein (BmDSCLP).

In this paper, we cloned the *BmDSCLP* gene sequence from silkworm pupa and expressed the target protein in *Escherichia coli*. Polyclonal anti-BmDSCLP antibodies were prepared to determine the subcellular localization of the protein. Finally, we determined the expression pattern of the *BmDSCLP* gene at different developmental stages and in different tissues of the fifth instar larva. We hope that these results will provide a foundation for future studies on the biological functions of the BmDSCLP protein.

MATERIALS AND METHODS

Animal materials, bacterial strains and reagents

E. coli strains TG1 and BL21 (DE3) were maintained in our laboratory. The *B. mori* strain was an offspring of Jingsong × Haoyue. Silkworms were reared using mulberry leaves under standard conditions. The heads, silk glands, guts, Malpighian tubules, testes, ovaries, fat bodies and epidermis of spinning silkworms were dissected, immediately frozen in liquid nitrogen and stored at -80°C. The larvae (day 8 of the fifth instar), pupae (day 6 after spinning), ovum and moth were also frozen in liquid nitrogen and stored at -80°C.

Bioinformatics analyses

Similarity analysis of nucleotide and protein sequences was carried out using the Basic Local Alignment Search Tool (BLAST)N (in the EST_others database) and BLASTP (in all non-redundant databases) algorithms in GenBank, respectively. The deduced amino acid sequence was analyzed with the expert protein analysis system (http://www.expasy.org/). The protein conformation was modeled by the SWISSMODEL program (http://swissmodel.expasy.org/) and viewed in the Swiss PDB viewer (Schwede et al., 2003). Multiple alignments of the Kazal domains were performed using the CLUSTAL-W program of the Bioedit software.

Construction of the recombinant plasmid

Total RNA was extracted from the tissues of spinning silkworms using the Trizol reagent (Invitrogen), according to the manufacturer's instructions. The ready-to-go T-primed first-strand kit (Amersham) was employed to synthesize first-strand cDNAs from total RNA. The first-strand cDNA was used as the template to amplify a fragment from the coding region by using polymerase chain reaction (PCR). PCR primers were designed using the primer premier 5.0 software. The PCR primers were based on the open reading frame (ORF) sequence and included the upper primer (5′-GCGGGATCCAT GCGGCCTCCCACGGAATATG-3′) and lower primer (5′-GCGCT CGAGTTAGAGTATGAGATCTTC-3′). The *Bam*HI and *Xho*I restriction sites were introduced in the primers. The PCR program consisted of a preliminary denaturation step at 94°C for 5 min, followed by 30 cycles of amplification (denaturation at 94°C for 1 min, annealing at 58°C for 45 s and extension at 72°C for 45 s) and a final extension at 72°C for 10 min. The PCR products were purified using the PCR rapid purification kit (BioDev-Tech, China). After digestion with *Bam*HI/*Xho*I (Promega), the fragments were cloned into the expression vector pET-28a and transformed into *E. coli* TG1 competent cells. A positive colony with the *BmDSCLP* gene in the plasmid was identified and confirmed by PCR, double digestion of the plasmid and sequencing on an ABI PRISM 3130XL system (Applied Biosystems).

Expression and purification of BmDSCLP

The recombinant plasmid pET-28a-BmDSCLP was transformed into *E. coli* BL21 (DE3)-star strain cells. Expression of the His-tagged fusion protein was induced by adding 1 mM isopropyl-β-d-thio-galactoside (IPTG) and continuing cell growth for 4 h. The bacteria were lysed by pulsed sonication in a UP200H cell disruptor (Dr. Heilscher, Germany) for 20 min on ice. Sodium dodecylsulfate-polyacrylamide gel electrophoresis (SDS-PAGE) analysis indicated that the recombinant BmDSCLP protein was in the form of inclusion bodies. The lysates were centrifuged at 14,000 × g for 30 min at 4°C to remove the supernatant and the precipitate was successively rinsed in washing buffer I (20 mM Tris with 1% Trion × -100) and washing buffer II (20 mM Tris with 2 M urea). The precipitate was then dissolved in a solubilizing buffer (20 mM Tris containing 6 M urea and 100 mM β-mercaptoethanol). After centrifugation, the supernatant containing the BmDSCLP protein was purified on HiTrap Chelating HP (Amersham), according to the manufacturer's instructions. The eluted BmDSCLP was desalted and concentrated in a Microcon YM-10 system (Millipore). The concentrated BmDSCLP was dissolved in solution A (5% acetonitrile containing 0.1% trifluoroacetic acid/water) and injected into a POROS 10 R1 reverse-phase fast protein liquid chromatography (FPLC) column (Amersham biosciences) that had been pre-equilibrated with solution A at a flow rate of 1 ml/min. A linear gradient of acetonitrile (from 5 to 95% (v/v)) in elution buffer was applied for 20 min. The absorbance was monitored at 280 nm and

the fractions were collected automatically. The eluted BmDSCLP was freeze-dried in an Alpha 2-4 freeze dryer (Christ) and then stored at -20°C.

Molecular weight determination

The molecular weight of BmDSCLP was assessed by SDS-PAGE on 12% polyacrylamide gels and confirmed using the Q-TRAP MS/MS system (Applied Biosystems). Purified BmDSCLP was dissolved to a final concentration of 100 pg/µl in 80% acetonitrile containing 0.1% (v/v) trifluoroacetic acid in water. The analyses were performed at the default settings for Turbospray and Q-TRAP parameters.

Preparation and purification of the anti-BmDSCLP serum

The freeze-dried fusion protein was redissolved in phosphate buffered saline (PBS) and quantitated by UV spectrophotometry using a NanoDrop ND-1000 system. A mixture containing 1 mg purified recombinant BmDSCLP and Freund's complete adjuvant (Dingguo) was intraperitoneally injected into a New Zealand white rabbit. The rabbit was boosted three times with 1 mg recombinant BmDSCLP in Freund's incomplete adjuvant at 1 week interval. Serum prepared from blood collected 10 days after the fourth injection was purified on HiTrap Protein A HP (Amersham), in accordance with the manufacturer's instructions. After filtering the immunoglobulin G (IgG) through Ultracel PLCHK (Millipore), purified anti-BmDSCLP IgG was dissolved in 50% glycerol and stored at -80°C.

Titer analysis and specificity evaluation of the polyclonal antibodies

Indirect enzyme-linked immunosorbent assay (ELISA) was used to detect the antibody titer with negative rabbit sera serving as the control. Western blot analysis was used to evaluate the specificity of the polyclonal antibodies using extracts of bacteria carrying the recombinant plasmid and the purified recombinant protein. Samples were separated by 10% SDS-PAGE and electrotransferred onto polyvinyl difluoridene (PVDF) membranes. After blocking in 3% non-fat milk in PBS at 4°C overnight, the membranes were probed with the rabbit anti-BmDSCLP antibody at room temperature for 3 h. After washing with PBST (0.1% Tween-20 in PBS), the membranes were incubated with anti-rabbit IR dye 700 and examined with infrared laser imaging system 9201F (Licor).

Subcellular localization of BmDSCLP

BmN cells were cultured overnight on glass cover slips, washed three times with PBS for 5 min each and fixed in PBS (pH 7.2) containing 3.7% polyformaldehyde at room temperature for 15 min. The fixed cells were blocked in 3% bovine serum albumin (BSA) in PBS at room temperature for 2 h, followed by three 10 min washes in PBST (0.05% Tween-20 in PBS). The cells were then incubated overnight at 4°C with antiserum containing anti-BmDSCLP polyclonal antibodies (diluted 1:500 in blocking buffer); the cells were also simultaneously incubated with negative serum as the control. The negative serum was obtained from the rabbit prior to immunization with the antigen. After three 10 min washing in PBST, the cells were incubated with Cy3-labeled goat anti-rabbit IgG (diluted 1:500; Promega) at 37°C for 2 h and then, washed twice for10 min each in PBST. The cells were then incubated with 4′-6-diamidino-2-phenylindole (1 g/ml in PBS) at room temperature for 10 min. After washing once with PBST, the cells were examined under a Nikon ECLIPSE TE2000-E Confocal microscope and the images were analyzed using EZ-C1 software.

RT-PCR expression analysis

To determine the tissue distribution expression profiles of the Bm-DSCLP gene, total RNA was extracted from the heads, Malpighian tubules, epidermis, silk glands, testis, guts, fat bodies and spiracle using the Trizol reagent (Invitrogen), according to the manufacturer's instructions. Contaminating genomic DNA was removed by DNase I (Invitrogen). The purity of extracted RNA was determined by UV spectrophotometry. The 260/280 nm ratios ranged between 1.8 and 2.1 for all RNA samples analyzed. The total RNA concentration was determined by measuring the absorbance at 260 nm using a SPECTRA max PLUS384 system (molecular devices).

The ReverTra Ace®qPCR RT kit (TOYOBO) was employed to synthesize first-strand cDNAs from total RNA. The first-strand cDNA was subjected to RT-PCR analysis using Real-time PCR master mix (SYBR Green) (TOYOBO) and an ABI 7300 real-time RT-PCR system (applied biosystems) with a specific primer pair for the *BmDSCLP* gene, 5′-TCTCAACCTATCAAACAACCA-3′ and 5′-AAT CTGTCCACATCAACTTCA-3′. As the control, a specific primer pair for the 18S *rRNA* gene, 5′-CGATCCGCCGACGTT ACTACA-3′ and 5′-GTCCGGGCCTGGTGAGATTT-3′, was used. The primer pairs were designed using the DNAStar software and were as follows: initial denaturation at 95°C for 1 min, followed by 40 cycles of denaturation at 95°C for 15 s, annealing at 51°C for 15 s and extension at 72°C for 45 s. The dissociation curve was determined by denaturation at 95°C for 15 s, 60°C for 30 s and 95°C for 15 s, to check for the presence of non-specific dsDNA SYBR green hybrids such as primer dimers. Fluorescence measurements were recorded during each extension step. At the end of each reaction, the data were automatically analyzed and amplification plots were obtained. Subsequently, the data were analyzed by the $-\Delta\Delta C_T$ method.

To determine the expression patterns of the *BmDSCLP* gene in various stages of *B. mori*, total silkworm RNAs from four different stages (egg, larva, pupa and moth) was subjected to real-time RT-PCR analysis using the procedures described earlier.

RESULTS

Sequence characteristics

The nucleotide sequence and the deduced amino acid sequence of the *BmDSCLP* gene (accession number FJ602779) are shown in Figure 1. The sequence analysis revealed that the ORF of the *BmDSCLP* gene was 642 bp long and encoded a putative protein of 213 amino acids. The predicted molecular mass was 24.05 kD and the theoretical isoelectric point was 5.19.

Similarity searches of the deduced protein against the non-redundant database of GenBank using the BLASTP program revealed significant homology to the death-associated small cytoplasmic leucine-rich protein

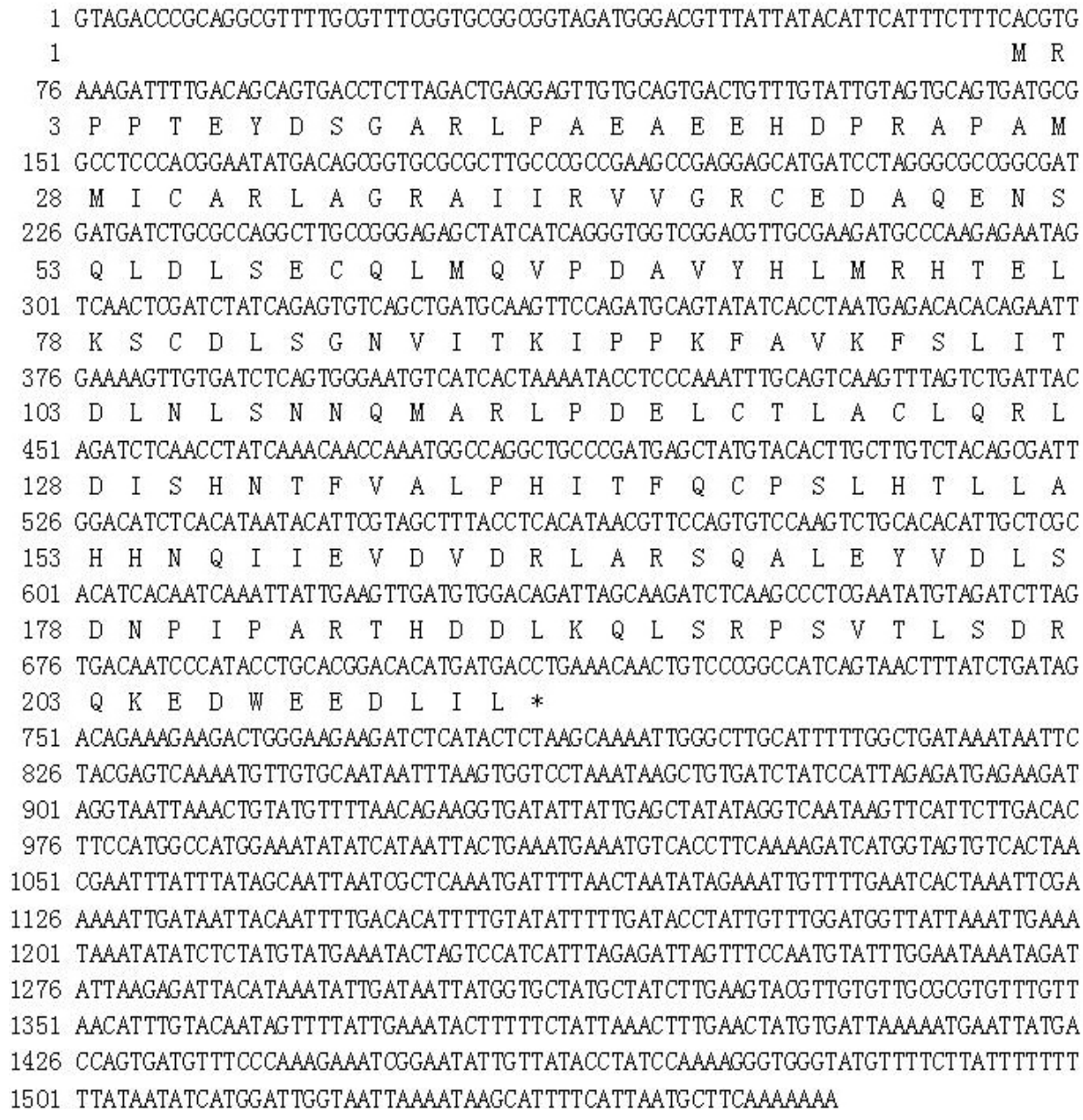

Figure 1. The nucleotide sequence and deduced amino acid sequence of the *BmDSCLP* gene (GenBank accession no. FJ602779). The asterisk (*) indicates the stop codon. The nucleotides and amino acids are numbered along the left margin.

(accession number AAF65467) from *Manduca sexta.* Since the homology between the two proteins was 93%, we named the protein discovered in this study BmDSCLP.

Sequence analysis revealed that, BmDSCLP contains two identical and conserved LRR domains (COG4886) and each domain contains 4 complete and 2 incomplete LRRs.

We employed the CLUSTAL-W program to generate multiple alignments of the sequence of BmDSCLP with those of nine DSCLP proteins from other organisms (Figure 2). Significant similarities were detected between BmDSCLP and other DSCLPs. The results showed that, the LRR sequences are highly conserved. Moreover, the homologies of these proteins were very high (48% above),

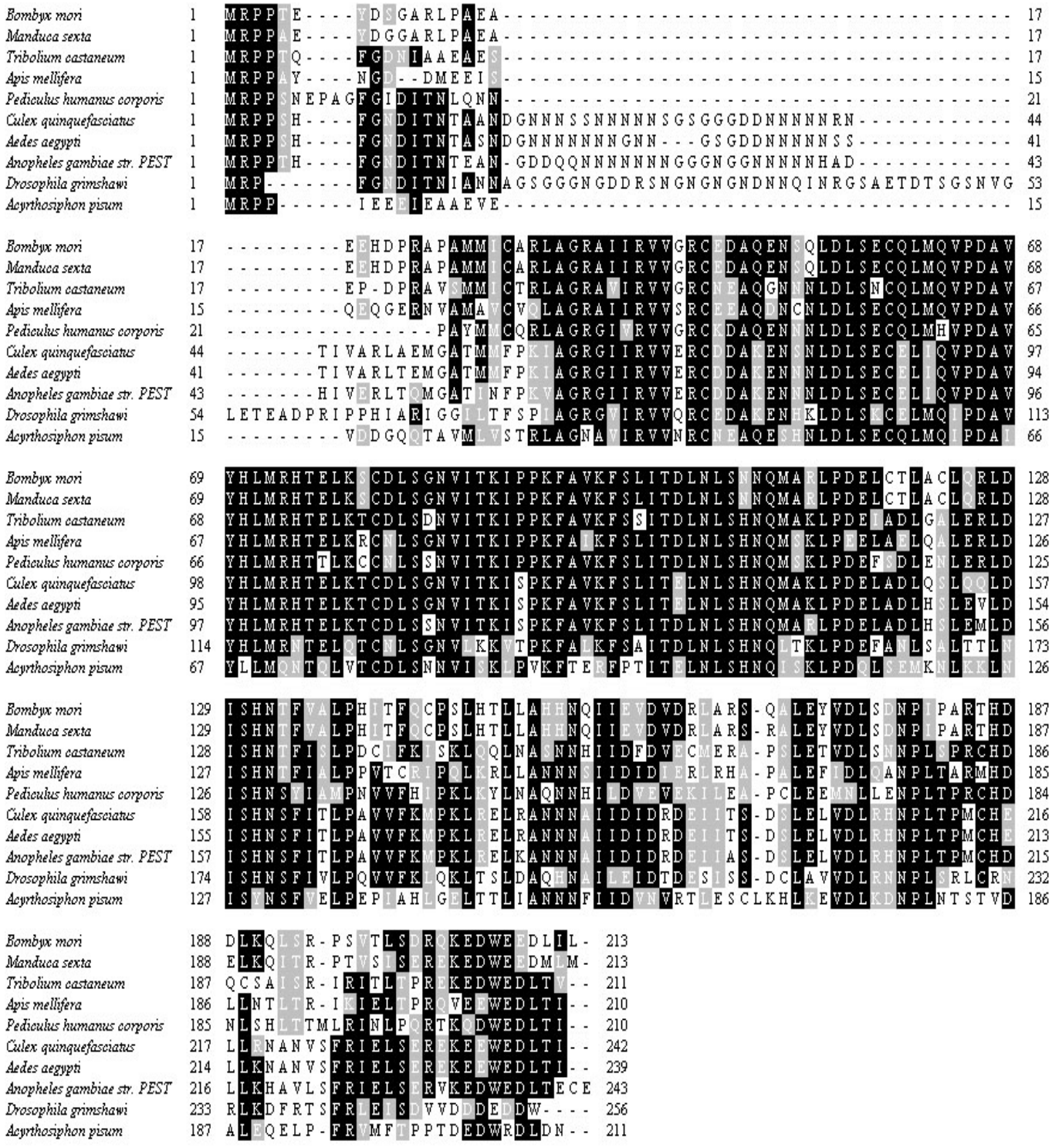

Figure 2. Alignment of the deduced amino acid sequence of BmDSCLP with the sequences of homologous proteins from other organisms, *B. mori* (accession no. FJ602779), *M. sexta* (accession no. AAF65467), *T. castaneum* (accession no. XP_967237), *A. mellifera* (accession no. XP_623853), *P. humanus corporis* (accession no. EEB17882), *C. quinquefasciatus* (accession no. XP_001846916), *A. aegypti* (accession no. XP_001648693), *A. gambiae str. PEST* (accession no. XP_312362), *D. grimshawi* (accession no. XP_001991875) and *A. pisum* (accession no. XP_001943937).

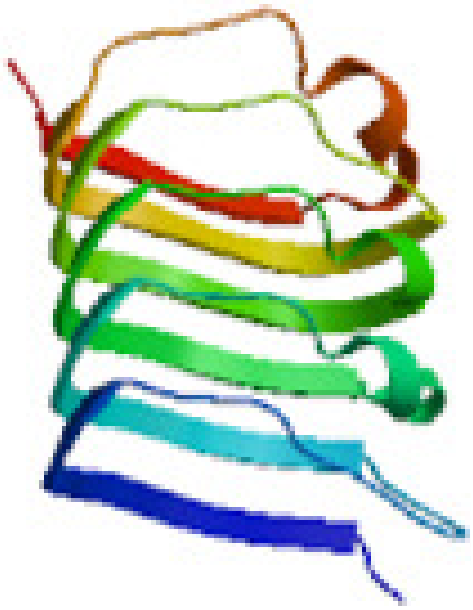

Figure 3. Deduced 3D structure of BmDSCLP.

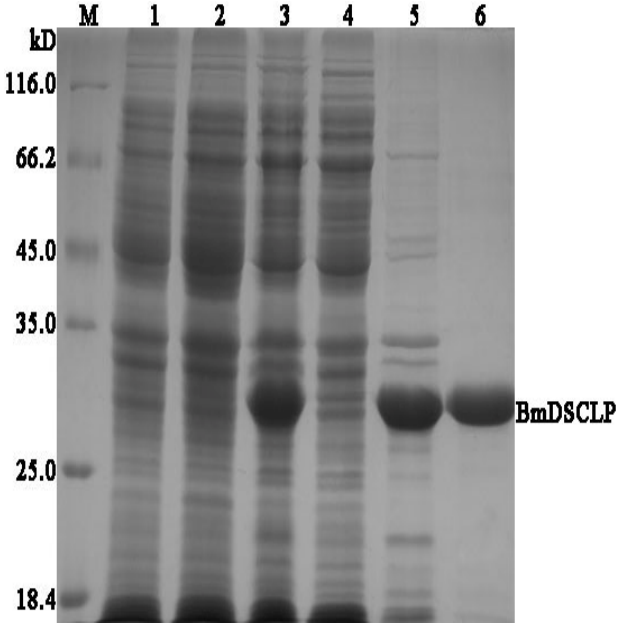

Figure 4. Expression and purification of recombinant BmDSCLP was analyzed by Coomassie blue staining of the SDS-PAGE gel. Lane M, protein mass markers; lane 1, lysate of the blank vector in *E. coli* BL21-Star cells after IPTG induction; lane 2, lysate of *E. coli* BL21-Star cells that were not induced; lane 3, lysate of *E. coli* BL21-Star cells after IPTG induction; lane 4, supernatant of *E. coli* BL21-star cells after IPTG induction; lane 5, pellet fraction of *E. coli* BL21-Star cells after IPTG induction; lane 6, eluate after His-affinity purification.

for instance, BmDSCLP had 93, 65, 62, 56, 61, 61, 63, 50 and 48% sequence identity to the sequences from *M. sexta* (accession no. AAF65467), *Tribolium castaneum* (accession no. XP_967237), *Apis mellifera* (accession no. XP_623853), *Pediculus humanus corporis* (accession no. EEB17882), *Culex quinquefasciatus* (accession no. XP_001846916), *Aedes aegypti* (accession no. XP_001648693), *Anopheles gambiae str. PEST* (accession no. XP_312362), *Drosophila grimshawi* (accession no. XP_001991875) and *Acyrthosiphon pisum* (accession no. XP_001943937).

The hypothetical conformation of BmDSCLP was predicted by the Swiss-model program (Figure 3). The results showed that BmDSCLP is composed of 6 β-sheets and 5 α-helices, similar to a barrel protein.

Expression and purification of recombinant BmDSCLP

The *BmDSCLP* ORF fragment (642 bp) encoding BmDSCLP was inserted into the expression vector pET-28a. The recombinant bacteria were ultrasonicated and the resulting homogenate was centrifuged. The supernatant and sediment were separated and collected for SDS-PAGE analysis. The results showed that the fusion protein was present in the form of inclusion bodies in the precipitate. After resolubilization of the inclusion bodies followed by Ni^{2+}-affinity chromatography, recombinant BmDSCLP was obtained in high purity, as confirmed by electrophoresis (Figure 4). FPLC analysis showed that the purity of the obtained BmDSCLP was higher than 95%.

We determined the molecular weight of the fusion protein by mass spectrometry. The obtained molecular weight of 27.74 kD (Figure 5) agreed well with the theoretical value of 27.61 kD (24.05 kD (the predicted molecular weight of the 642 bp fragment) + 3.56 kD (the molecular weight of the His tag)).

Titer analysis and specificity determination of polyclonal antibodies

After obtaining all the extinction values, we used ELISA to determine the following ratio for antibodies against BmDSCLP; positive serum extinction value/negative serum extinction value (P/N) ≥ 2.1 was considered to be positive; 1.5 ≤ P/N < 2.1, doubtful and P/N < 1.5, negative. Based on this, the antibody titer was found to be higher than 1:12800 at a concentration of 10 μg/ml. We used western blots to determine the specificity of the polyclonal antibodies produced. The antibody reacted with a protein from the total lysates of induced *E. coli* and with

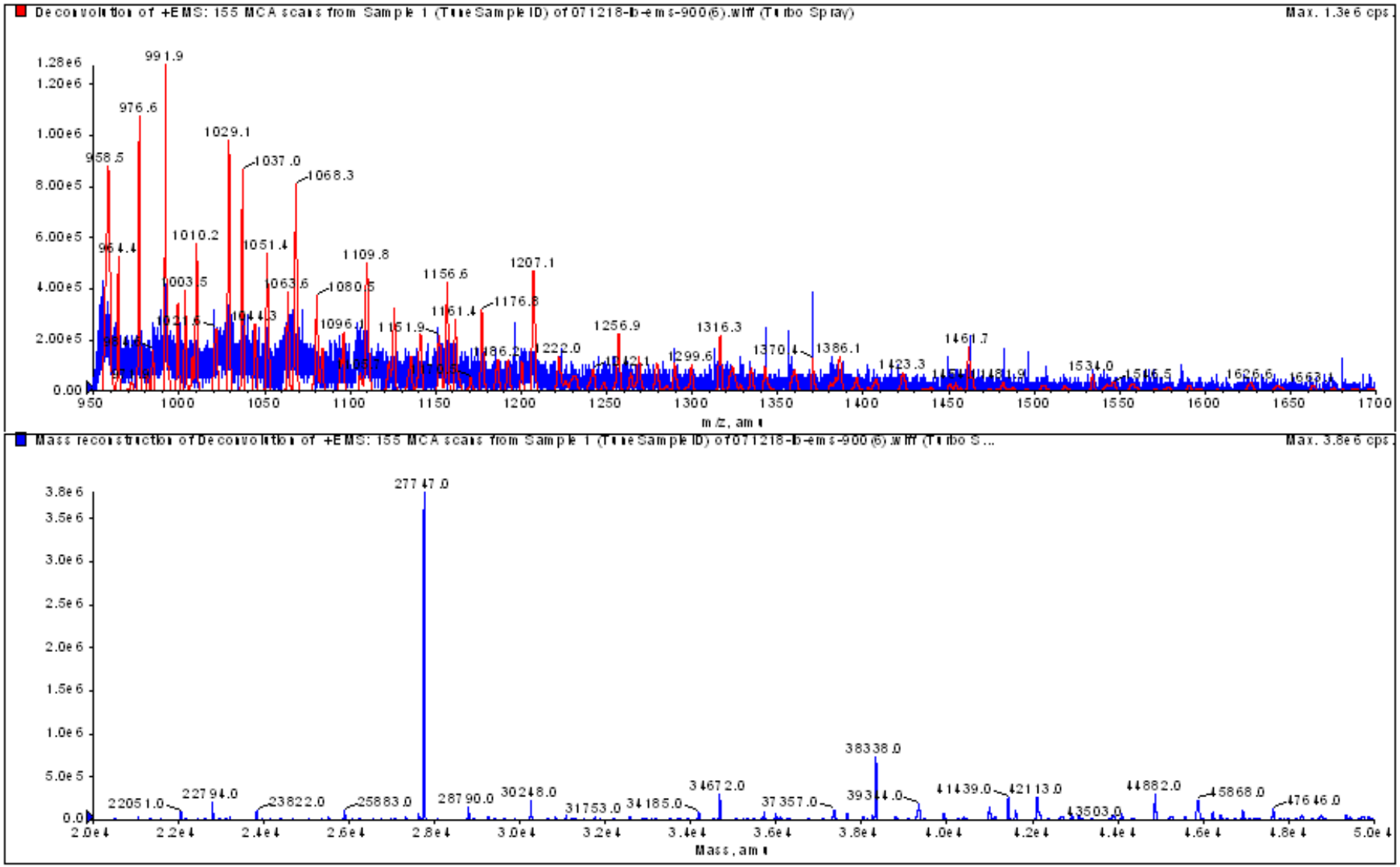

Figure 5. Analysis of the His-tagged fusion protein by MS.

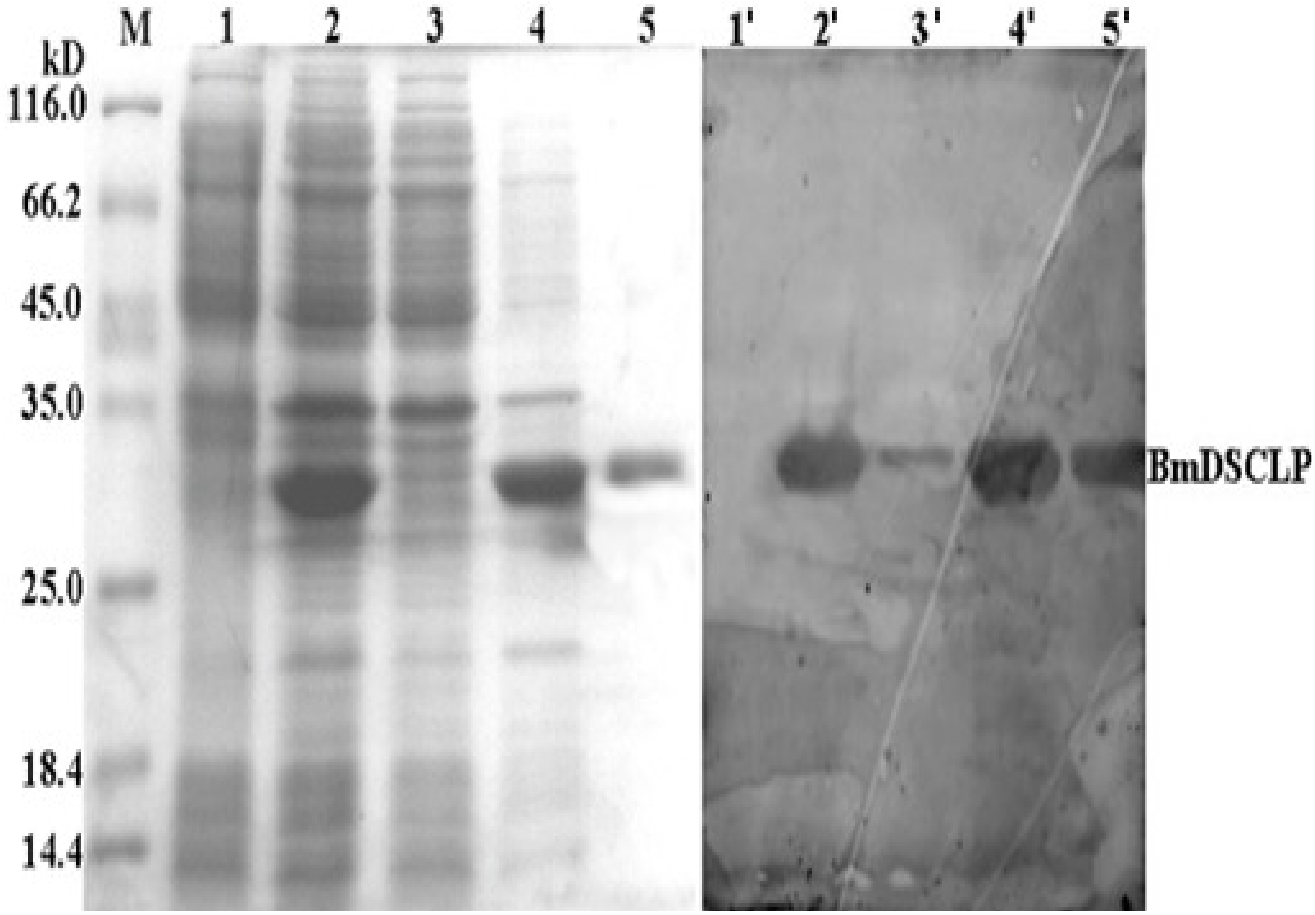

Figure 6. Western blot of the His-tagged fusion protein expressed in *E. coli* BL21. Lane M, protein mass markers; lane 1, lysate of *E. coli* BL21-Star cells that were not induced; lane 2, lysate of *E. coli* BL21-Star cells after IPTG induction; lane 3, supernatant from *E. coli* BL21-Star cells after IPTG induction; lane 4, pellet fraction of *E. coli* BL21-Star cells after IPTG induction; and lane 5, eluate after His-affinity purification. Lanes 1′ to 5′ in the western blot correspond to lanes 1 to 5, respectively, in the gel.

purified BmDSCLP of molecular weight only 27.7 kD (Figure 6), whereas no signal was detected in the non induced *E. coli* extract. These results illustrated the high specificity of the polyclonal antibodies.

Subcellular localization of BmDSCLP

The treated cells were examined under a Nikon ECLIPSE TE2000-E Confocal microscope and the images were analyzed using the EZ-C1software. Cy3-labeled goat anti-rabbit IgG emit red fluorescence when stimulated with light of wavelength 550 nm and DAPI-stained nuclei emit red fluorescence when stimulated with light of wavelength 353 nm. Our results indicated that, BmDSCLP was localized in both the cytoplasm and nucleus but was primarily found in the cytoplasm (Figure 7).

Expression pattern of the *BmDSCLP* gene during different developmental stages

To determine the transcription levels of the *BmDSCLP* gene at various developmental stages in the silkworm, we extracted total RNAs from the silkworm egg, fifth instar larva, pupa and moth. We performed real-time RT-PCR analyses on the mRNA extracts to determine the *BmDSCLP* transcription levels. The results from the melting curve analysis (data not shown) suggested that, no overt primer dimers were formed during PCR amplification. The amplification curves (data not shown) showed good reproducibility across repetitions. Our PCR

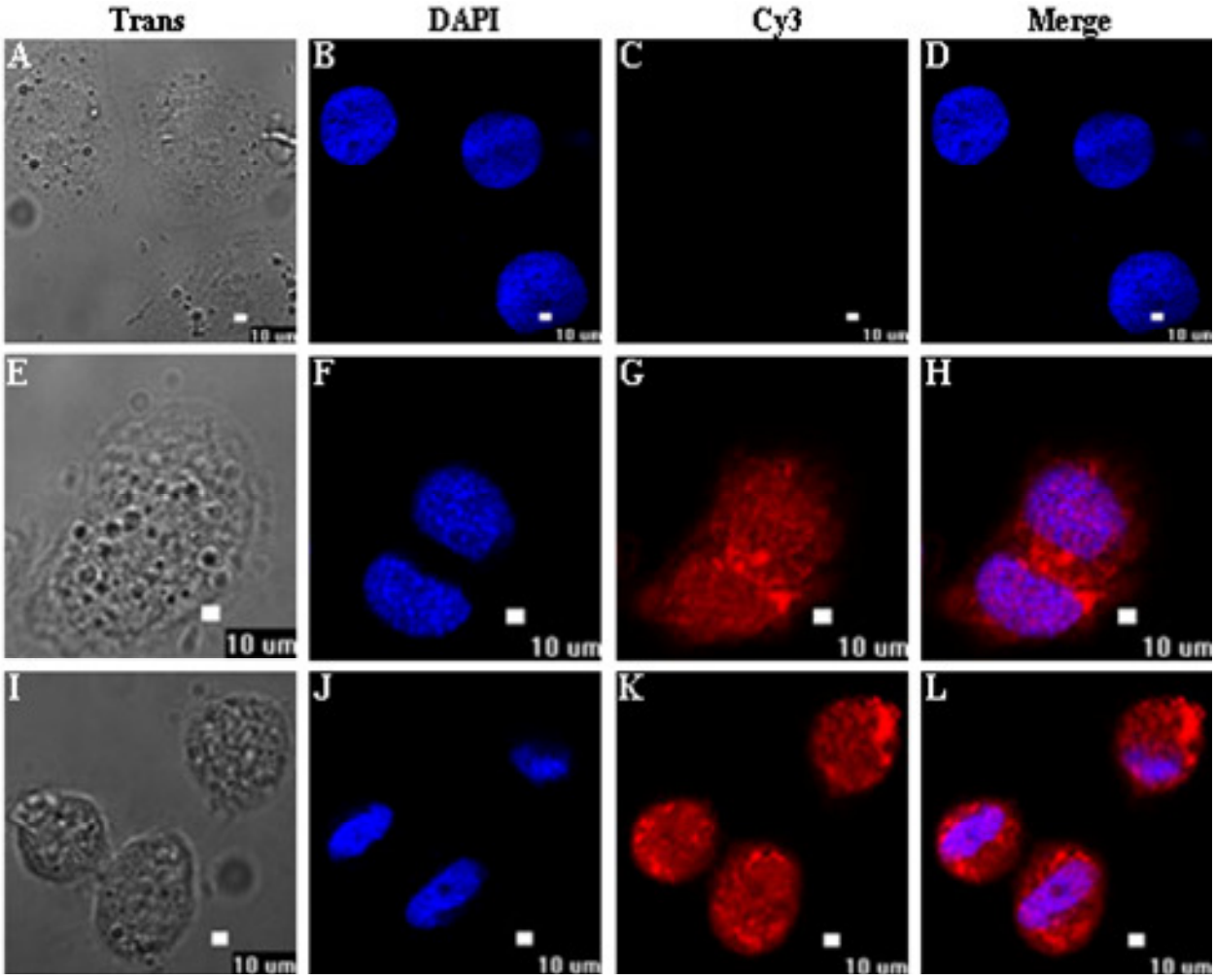

Figure 7. Subcellular localization of BmDSCLP with Cy3-labeled goat anti-rabbit IgG and DAPI. A to D, the negative control group using negative rabbit serum; E to H and I to L, experimental group using the anti-BmDSCLP polyclonal antibody. A, E and I: the cell under transmitted light; B, F, J, DAPI staining; C, G, K, BmDSCLP subcellular localization as indicated by the Cy3-labeled secondary antibody; D, H, L, merged image. Scale bars represent 10 μm.

results indicated an obvious difference in the *BmDSCLP* transcription levels of the four developmental stages (Figure 8). The transcription level of the *BmDSCLP* gene was highest in the moth and lowest in the egg.

Tissue distribution of the *BmDSCLP* gene in the fifth instar larva

To determine the transcriptional levels of the *BmDSCLP* gene in these tissues, we isolated the total RNAs from the fifth instar larva tissues and used it to perform real-time RT-PCR. Our results showed that, *BmDSCLP* mRNA was most abundant in the testis; less abundant in the head, epidermis, Malpighian tubules, spiracle, fat body, and midgut and least abundant in the silk glands (Figure 9).

DISCUSSION

We cloned the *BmDSCLP* gene from silkworm pupa using bioinformatics and RT-PCR methods and expressed the target protein in *E. coli*. After purification by His-affinity chromatography and FPLC, the recombinant protein was used to raise polyclonal antibodies that were then, used to determine the subcellular localization of the native protein. We also analyzed the expression patterns of the *BmDSCLP* gene at different developmental stages and in

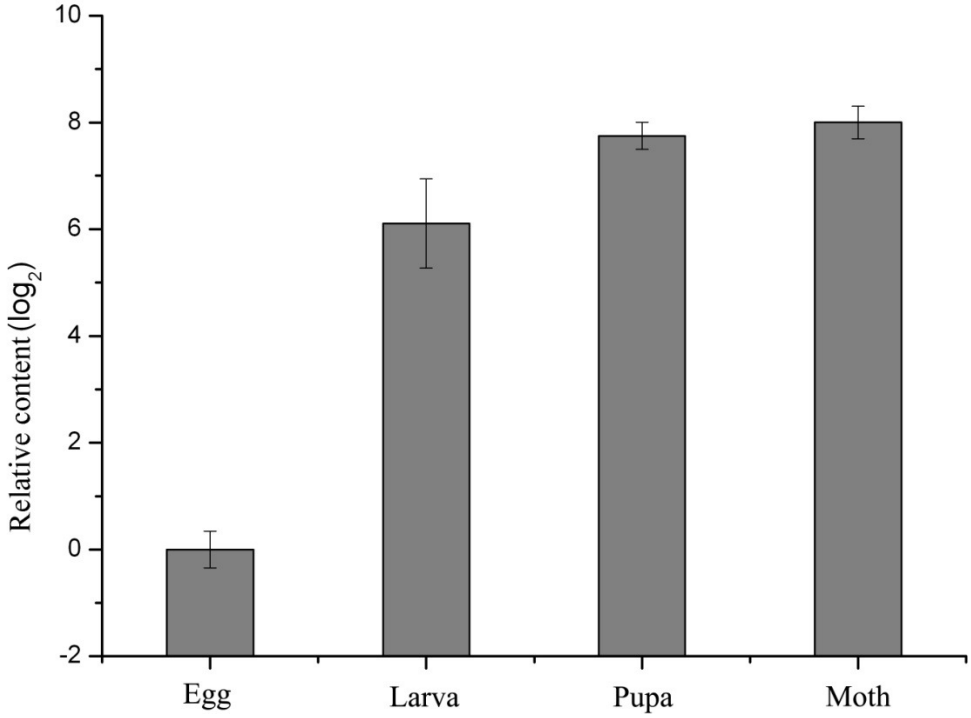

Figure 8. Transcription patterns of the *BmDSCLP* gene during different developmental stages of *B. mori*. The relative *BmDSCLP* expression was determined in relation to the corresponding *BmDSCLP* expression level in the silkworm egg: $\Delta\Delta C_{T(stage)} = \Delta C_{T\ (stage)} - \Delta C_{T(egg)}$; the y-axis log2 value is equal to $\Delta\Delta C_T$. Number of experiments performed was 3, and the error bar indicates the SD.

different tissues of the fifth instar larva by using RT-PCR. BLASTP analysis showed that, the homology between the BmDSCLP protein and the DSCLP protein of *A. aegypti* was as high as 93%; the high homology suggests that these proteins have the same or similar biological functions. A study of the abdominal section of adult *A. aegypti* showed that, DSCLP can promote cell apoptosis (Kuelzer et al., 1999). Moreover, DSCLP contains 4 complete and 2 incomplete LRR sequences and had a molecular weight of approximately 24 kD. This was very similar to the structure and molecular weight of BmDSCLP, indicating that BmDSCLP may also play a role in promoting apoptosis. Using western blot analysis, Kuelzer et al. (1999) also examined DSCLP expression in the larvae and pupa of *A. aegypti* and found that, the protein was expressed at high levels in the testis and Malpighian tubules of the larval stage, while no expression was detected in the egg and adult stage (Kuelzer et al., 1999). This is not consistent with the BmDSCLP expression patterns in different developmental stages and different tissues of the fifth instar larvae as detected by RT-PCR. One possible reason is that, there are some differences between species in terms of gene transcription and protein expression or that protein expression is also affected by post-translational regulation. Studies on functional differences of the same protein from different species could provide a better understanding of protein function.

The intensities of the protein bands on the PVDF membrane in western blotting were higher than those on the SDS-PAGE gel. A possible explanation is that the proteins may have penetrated the PVDF membrane because the latter had been immersed in liquid for a long time. Although, the SDS-PAGE results indicated that the protein may only be in the form of inclusion bodies, the western blot results showed that recombinant BmDSCLP was also present in the supernatant.

Wang et al. (2003) used immunohistochemical analysis to prove that DSCLP is a cytoplasmic protein. There were some differences in the experimental results obtained from silkworm BmN cells. LRR proteins are located in the nucleus, cytoplasm, plasma membrane and extracellular matrix (Buchanan and Gay, 1996). One possible reason is that, the specificity of polyclonal antibodies was not very high, as a result of which the protein was also detected in the nucleus. Another possible reason is that, there

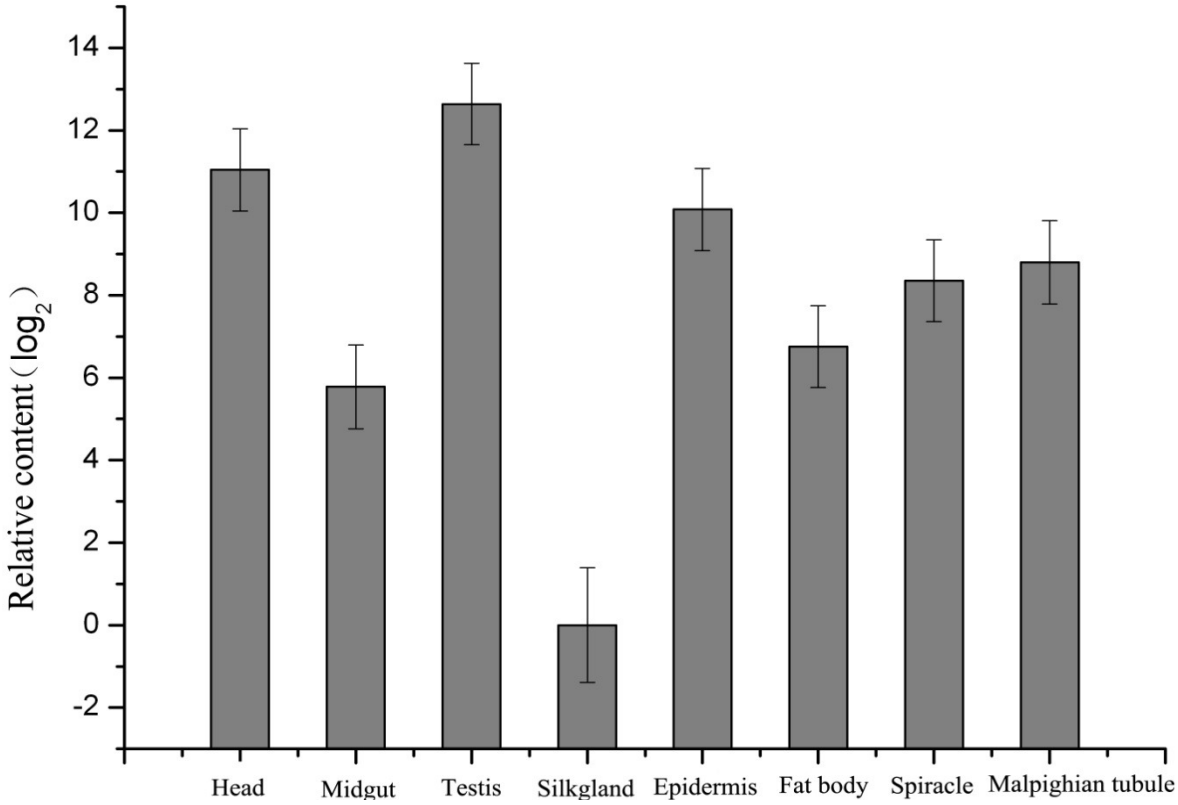

Figure 9. Transcription levels of the *BmDSCLP* gene in different tissues of the fifth instar larva of *B. mori*. Relative *BmDSCLP* expression was determined in relation to the corresponding *BmDSCLP* expression level in the silk gland: $\Delta\Delta C_{T\,(tissue)} = \Delta C_{T\,(tissue)} - \Delta C_{T\,(silk\ gland)}$; the y-axis log2 value is equal to $\Delta\Delta C_T$. The number of experiments was 3, and the error bar indicates the SD.

are inherent differences in the distribution of the protein across different species. Our study showed that, the *BmDSCLP* gene is expressed at different developmental stages in the silkworm, suggesting that BmDSCLP may play a very important role in the life cycle of *B. mori*. The testis is the reproductive organ of silkworms and the *BmDSCLP* gene showed a high level of transcription in the silkworm testis, indicating that its expression may be related to reproductive development in the silkworm. We also found that, gene transcription was the highest during the adult stage. The adult stage is the egg-laying period of repro- duction and this is a further indicator of the role of this protein in reproductive development.

ACKNOWLEDGMENTS

This study was supported by grants from the National High Technology Research and Development Program (nos. 2007AA021703 and 2007AA100504), the Zhejiang Natural Science Foundation (nos. Y3080183 and Y3090176) and the Zhejiang Open Foundation of the Most Important Subjects (no. SWYX0909).

REFERENCES

Buchanan SG, Gay NJ (1996). Structural and functional diversity in the leucine-rich repeat family of proteins. Prog Biophys Mol. Biol. 65(1-2): 1-44.

Dixon MS, Jones DA, Keddie JS, Thomas CM, Harrison K, Jones JD (1996). The tomato Cf-2 disease resistance locus comprises two functional genes encoding leucine-rich repeat proteins. Cell. 84(3): 451-459.

Draper MP, Liu HY, Nelsbach AH, Mosley SP, Denis CL (1994). CCR4 is a glucose-regulated transcription factor whose leucine-rich repeat binds several proteins important for placing CCR4 in its proper promoter context. Mol. Cell Biol. 14(7): 4522-4531.

Haberland J, Gerke V (1999). Conserved charged residues in the leucine-rich repeat domain of the Ran GTPase activating protein are required for Ran binding and GTPase activation. Biochem J. 343(3): 653-662.

Kobe B, Deisenhofer J (1995). A structural basis of the interactions between leucine-rich repeats and protein ligands. Nature, 374(6518): 183-186.

Kobe B, Deisenhofer J (1994). The leucine-rich repeat: a versatile

binding motif. Trends Biochem. Sci. 19(10): 415-421.
Kobe B, Deisenhofer J (1993). Crystal structure of porcine ribonuclease inhibitor, a protein with leucine-rich repeats. Nature, 366(6457): 751-756.
Kobe B, Deisenhofer J (1996). Mechanism of ribonuclease inhibition by ribonuclease inhibitor protein based on the crystal structure of its complex with ribonuclease A. J. Mol. Biol. 264(5): 1028-1043.
Kobe B, Kajava AV (2001). The leucine-rich repeat as a protein recognition motif. Curr. Opin. Struct. Biol. 11(6): 725-732.
Kuelzer F, Kuah P, Bishoff ST, Cheng L, Nambu JR, Schwartz LM (1999). Cloning and analysis of small cytoplasmic leucine-rich repeat protein (SCLP), a novel, phylogenetically-conserved protein that is dramatically up-regulated during the programmed death of moth skeletal muscle. J. Neurobiol. 41(4): 482-494.
Kuja-Panula J, Kiiltomaki M, Yamashiro T, Rouhiainen A, Rauvala H (2003). AMIGO, a transmembrane protein implicated in axon tract development, defines a novel protein family with leucine-rich repeats. J. Cell Biol. 160(6): 963-973.
Medzhitov R, Preston-Hurlburt P, Janeway Jr. CA (1997). A human homologue of the *Drosophila* Toll protein signals activation of adaptive immunity. Nature, 388(6640): 394-397.
Nose A, Takeichi M, Goodman CS (1994). Ectopic expression of connectin reveals a repulsive function during growth cone guidance and synapse formation. Neuron. 13(3): 525-539.
Patthy L (1987). Detecting homology of distantly related proteins with consensus sequences. J Mol Biol. 198(4): 567-577.
Rose D, Zhu X, Kose H, Hoang B, Cho J, Chiba A (1997). Toll, a muscle cell surface molecule, locally inhibits synaptic initiation of the RP3 motoneuron growth cone in *Drosophila*. Development, 124(8): 1561-1571.
Roth GJ (1991). Developing relationships: arterial platelet adhesion, glycoprotein Ib, and leucine-rich glycoproteins. Blood, 77(1): 5-19.
Schwede T, Kopp J, Guex N, Peitsch MC (2003). SWISS-MODEL: An automated protein homology-modeling server. Nucleic Acids Res. 31(13): 3381-3385.
Tensen CP, Van Kesteren ER, Planta RJ, Cox KJ, Burke JF, van Heerikhuizen H, Vreugdenhil E (1994). A G protein-coupled receptor with low density lipoprotein-binding motifs suggests a role for lipoproteins in G-linked signal transduction. Proc. Natl. Acad. Sci. USA. 91(11): 4816-4820.
Wang W, Yang Y, Li L, Shi Y (2003). Synleurin, a novel leucine-rich repeat protein that increases the intensity of pleiotropic cytokine responses. Biochem. Biophys. Res. Commun. 305(4): 981-988.
Wu W, Wong K, Chen J, Jiang Z, Dupuis S, Wu JY, Rao Y (1999). Directional guidance of neuronal migration in the olfactory system by the protein Slit. Nature, 400(6742): 331-336.